Arch. Metall. Mater. **65** (2020), 1, 175-183

DOI: 10.24425/amm.2019.131112

P. KWOLEK[1*]

EFFECT OF Na_3VO_4 INHIBITOR ON THE CORROSION RESISTANCE OF Al_2Cu INTERMETALLIC PHASE IN H_3PO_4 AQUEOUS SOLUTION

Sodium orthovanadate was tested as a corrosion inhibitor of intermetallic Al_2Cu in 1 M H_3PO_4. The Al_2Cu – H_3PO_4 – Na_3VO_4 system was studied using the following methods: inductively coupled plasma optical emission spectrometry, scanning electron microscopy with energy dispersive x-ray spectroscopy, x-ray diffraction, electrochemical impedance spectroscopy, polarisation and open circuit potential. It was found that the corrosion rate decreased as the inhibitor concentration increased. The highest inhibition efficiency 99% was obtained when sodium orthovanadate initial concentration was equal to 100 mM, pH = 1.11, due to precipitation of a protective layer of insoluble salt, containing vanadium, phosphorus, sodium and oxygen, on the surface. At pH = 0.76 the protective layer was not formed and inhibition efficiency decreased to 76%. Selective corrosion of the intermetallic phase caused a significant increase of an electric double layer capacitance and decrease of a charge transfer resistance.

Keywords: intermetallic phase; selective corrosion; orthophosphoric acid; electrochemical impedance spectroscopy; sodium orthovanadate

1. Introduction

Aluminium wrought and cast alloys, containing copper as the major alloying element, are commonly applied in industry. They achieve good mechanical properties after appropriate heat treatment which is precipitation hardening. Copper is then precipitated from a supersaturated solid solution as intermetallics Al_2Cu and Al_2CuMg, when the alloy contains also magnesium. These phases ensure good strength of the alloys but also deteriorate their corrosion resistance [1]. A strong galvanic coupling between the intermetallics and the matrix is responsible for that [2,3].

The corrosion resistance of aluminium and its alloys in aqueous solutions is related to a chemical stability of an aluminium oxide. Since Al_2O_3 dissolves in acidic solutions, aluminium alloys are not corrosion resistant in such an environment. Thus, components made of aluminium alloys are generally not used in acidic media. However, the corrosion resistance of aluminium in such solutions is required in some industrial processes. A good example is stripping of anodic coatings in hot orthophosphoric acid for gravimetric determination of the coating weight. In this case, chromium trioxide is commonly used as a corrosion inhibitor for the metallic substrate [4]. However, due to its toxicity, new, environmentally-friendly inhibitors must be developed. Sodium molybdate Na_2MoO_4 is potentially attractive replacement for hexavalent chromium. Molybdate anions in acidic solutions exist as isopoly- and heteropolyoxomolybdates. The latter are formed in solutions containing addenda atoms such as e.g. P, As and Si [5]. They can be easily reduced to phosphomolybdenum blue species. Heteropolyoxomolybdate and phosphomolybdenum blue species inhibit the corrosion of aluminium while copper-rich aluminium alloys to the lesser extent [6-9]; moreover they affect the dissolution rate of anodic coating [10].

Another promising metal, forming iso- and heteropolyoxoanions, is vanadium. Isopolyoxovanadates were studied as the corrosion inhibitors of 2024 aluminium alloy [11-15]. It was found that tetrahedrally-coordinated species such as $H_2VO_4^-$ and $V_4O_{12}^{4-}$ inhibit the cathodic process in the corrosion cell, in the mild-acidic, chloride-containing solutions [12]. The most well-known heteropoly species existing in Na_3VO_4 – H_3PO_4 system are $PV_{14}O_{42}^{9-}$ and $H_6PV_{13}O_{41}^{7-}$ and they have never been tested as the corrosion inhibitors of aluminium.

Copper-rich aluminium alloys are often anodised to improve their corrosion and wear resistance. Therefore, development of the new inhibitors requires understanding their influence on

[1] RZESZÓW UNIVERSITY OF TECHNOLOGY, FACULTY OF MECHANICAL ENGINEERING AND AERONAUTICS, DEPARTMENT OF MATERIALS SCIENCE, 2 WINCENTEGO POLA STR., 35-959 RZESZÓW, POLAND

* Corresponding author: pkwolek@prz.edu.pl

the corrosion behaviour of intermetallic phases and matrix in aluminium alloys in acidic solutions. In this work, the corrosion behaviour of Al_2Cu phase in 1 M H_3PO_4 – Na_3VO_4 system is discussed for the first time.

2. Experimental

Al_2Cu specimens were obtained by an electric arc melting process of Al and Cu (99.999 wt% purity, Alfa Aesar) under an Ar atmosphere (p = 60 kPa). Subsequently, they were annealed in air (T = 823 K, t = 30 h) to dissolve small amount of eutectic mixture of Al_2Cu and Al(Cu) solid solution crystals obtained during crystallisation. The phase composition of the electrodes was then confirmed using X-ray diffraction (ARL X'Tra X-ray diffractometer, Cu K_α radiation source). All the diffraction lines were ascribed to Al_2Cu phase, ICDD card no 04-001-0923. The specimens were cut using an electrical discharge machine, mounted in an epoxy resin, abraded by an emery paper (grit 320 and 500), washed with water, isopropyl alcohol, and then air-flow dried. The surface area of the electrodes was approximately 0.79 cm^2.

The influence of the initial concentration of sodium orthovanadate Na_3VO_4 (c_{inh} = 10, 50 and 100 mM) on the corrosion kinetics of intermetallic Al_2Cu was studied in 100 cm^3 of 1 M H_3PO_4, in equilibrium with air, T = 303 K. Concentrations of aluminium and copper were determined after 10 h immersion using inductively coupled plasma-optical emission spectroscopy ICP-OES (Ultima 2 Horiba Jobin Yvon) and the corrosion rate was calculated. Since the pH of the orthophosphoric acid solution (0.76) increases upon dissolution of Na_3VO_4, the corrosion rate of Al_2Cu phase was also studied for c_{inh} = 100 mM acidified with concentrated H_2SO_4 solution to pH = 0.76.

Electrochemical tests were performed using a Bio-Logic SP-300 potentiostat in a conventional 3-electrode electrochemical cell with a water jacket; the cell was placed in a Faraday cage. Platinum wire (20 cm^2) was applied as the counter electrode, Ag|AgCl (3 M KCl) as the reference electrode. It was placed in a Luggin capillary filled with 1 M KNO_3 solution.

The first stage in the electrochemical characterisation of the corrosion process was determination of an open circuit potential (OCP). It was measured for 20 min, than the first impedance spectrum was recorded. The subsequent ones were obtained every 2 h, between them the OCP was recorded. The impedance spectra were obtained in the frequency domain between 200 kHz and 10 mHz. The root mean square value of the sinusoidal perturbation was 5 mV. The impedance spectra were validated using a Kramers-Kronig transformation (KK Test software) [16,17]. Only spectra obtained under stationary conditions ($t \geq 159$ min) are presented in this work. They were approximated using the appropriate equivalent circuit (vide infra) in Zview software (Scribner Associates). The anodic and cathodic polarisation curves were determined using potentiodynamic method. They were obtained separately, starting from the OCP value obtained after t = 159 min, with the scanning rate 10 mV min^{-1}. Cathodic polarisation curves were also determined in solutions deaerated with argon.

The morphology and chemical composition of the surface of corroded Al_2Cu specimens were investigated using the scanning electron microscope (SEM) Phenom XL equipped with an energy-dispersive X-ray spectrometer (EDX). EDX method cannot determine an oxygen content in the specimen quantitatively since the stoichiometry of oxides, formed on the surface, remains unknown. Therefore, the oxygen content was only ranked as low, medium and high (Table 1).

3. Results and discussion

3.1. Corrosion rate

Al_2Cu phase in aqueous solutions is passive in the wide range of pH (2-12) [18]. However, since aluminium is less noble than copper, the intermetallic is susceptible to a selective corrosion beyond the aforementioned pH range. Aluminium atoms are preferentially dissolved and their concentration in the solution is much higher when compared to copper concentration. This was observed, when concentration of Na_3VO_4, c_{inh}, was 0 and 10 mM. (Fig. 1a). At the same time, surface of the electrode becomes porous and enriched with copper. It contains also a small amount of aluminium and oxygen (spot 1 in Fig. 2a and b, Table 1). The chemical composition of the electrode in the areas, where the porous layer peeled off, was close to that of Al_2Cu phase (spot 2 in Fig. 2a and b, Table 1). However, a lot of pits, where dealloying process starts, is visible there (Fig. 2b and f); an oxide phase can also be found (spot 3 in Fig. 2a and b, Table 1).

When c_{inh} = 50 mM, concentration of aluminium and copper in the solutions were comparable (Fig. 1a) and the surface of Al_2Cu phase was enriched with copper to the lesser extent. However, a small amount of vanadium and phosphorus were found on the surface, together with oxygen (spot 2 in Fig. 2c, Table 1). In addition, insoluble salt containing vanadium and phosphorus precipitated in the form of rose plants near the areas where intensive corrosion occurred (Fig. 2c, spot 1 and g, Table 1).

When c_{inh} = 100 mM, concentrations of aluminium and copper were the lowest among studied solutions. The surface of intermetallic Al_2Cu, was covered with a compact layer of corrosion product containing vanadium, phosphorus, sodium and oxygen (Fig. 2d, h).

It should be note here that sodium orthovanadate, when dissolved in acidic solution, can raise its pH according to equation :

$$pH^+ + qVO_4^- = H_xV_qO_y^{n-} + (4q - y)H_2O \qquad (1)$$

where p, q, x, y and n are the stoichiometric coefficients and their values depend on the pH and the total concentration of vanadium in the solution [5]. The pH of 1 M H_3PO_4 solution was 0.76 and did not change after addition of 10 mM Na_3VO_4. However, when c_{inh} was equal to 50 and 100 mM, pH increased to 0.88 and 1.11 respectively. Although the solution was still highly acidic, the pH

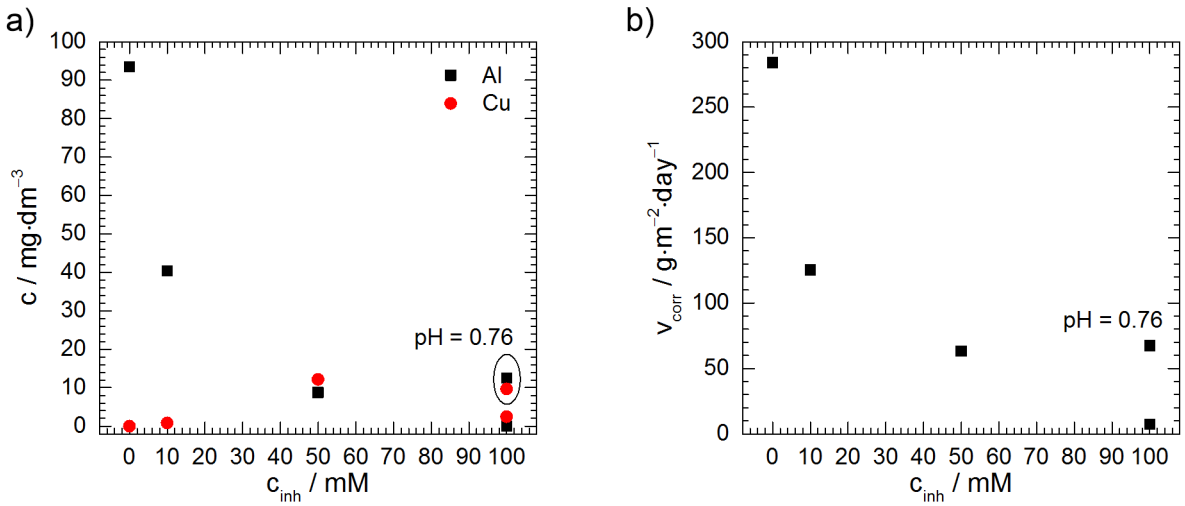

Fig. 1. Corrosion kinetics of Al_2Cu in 1 M H_3PO_4, T = 303 K: a) concentrations of aluminium and copper in the solution and b) corrosion rate

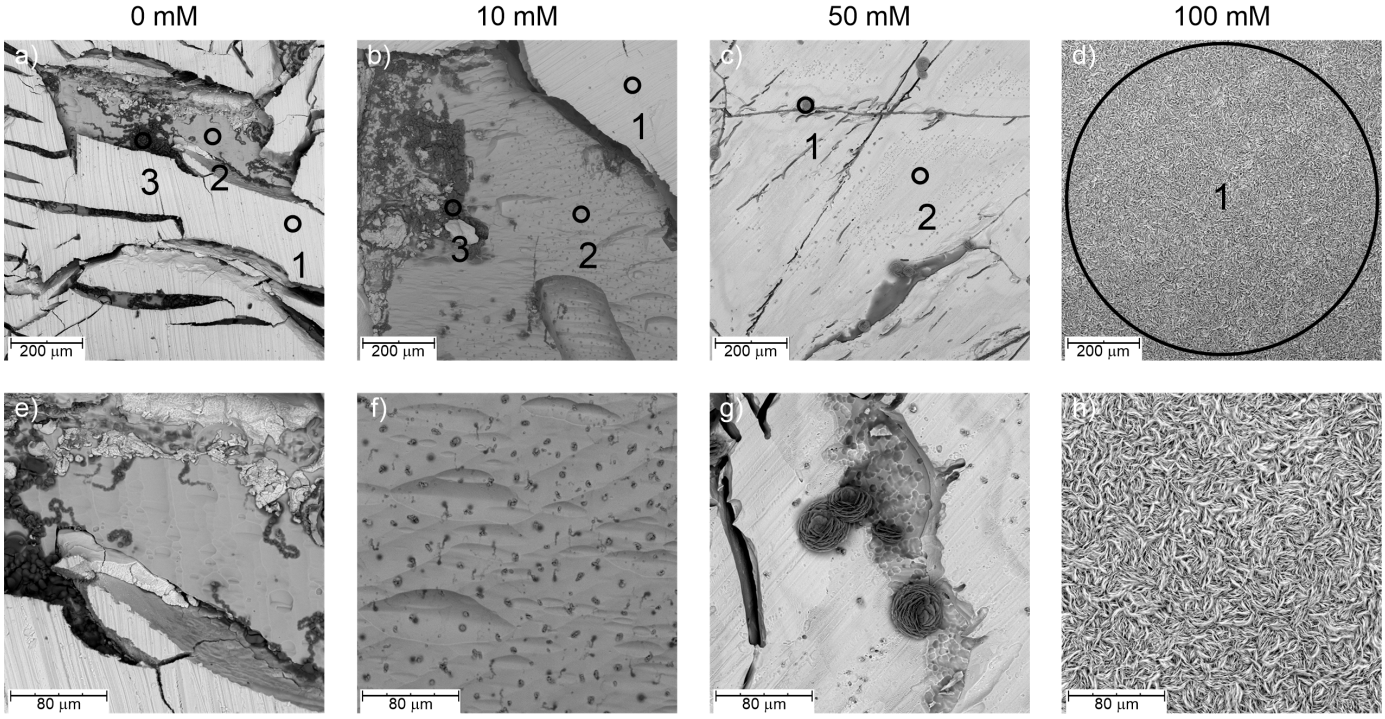

Fig. 2. Scanning electron micrograph of the Al_2Cu surface after 10 h exposure in 1 M H_3PO_4 as the function of initial concentration of Na_3VO_4, T = 303 K

TABLE 1

Chemical composition of the selected areas in Fig. 1, oxygen content was ranked as low +, medium ++ and high +++

c_{inh}, mM	Area in Fig. 1	Concentration of the elements, at.%						
		Cu	Al	O	V	P	Cl	Na
0	1	92.6 ± 4.0	7.4 ± 4.0	+				
	2	27.9 ± 2.1	72.1 ± 2.2	+				
	3	14.7 ± 1.1	85.3 ± 4.2	+++				
10	1	91.3 ± 3.9	8.7 ± 0.9	+				
	2	31.6 ± 4.1	64.6 ± 3.4	++		1.1 ± 0.2	2.7 ± 0.1	
	3	16.4 ± 0.9	81.1 ± 3.7	+++		0.9 ± 0.1	1.6 ± 0.2	
50	1	38.4 ± 2.3	21.6 ± 2.8	++	32.8 ± 3.3	7.2 ± 2.1		
	2	60.8 ± 2.1	34.8 ± 2.7	+	0.5 ± 0.1	3.9 ± 0.2		
100	1			+++	39.3 ± 2.2	41.2 ± 3.1		19.5 ± 1.1

change might affect the kinetics of corrosion. Therefore the additional experiment was performed, where the pH of the solution containing 100 mM of Na_3VO_4 was decreased from 1.11 to 0.76 using concentrated H_2SO_4. Solution acidification increased the concentrations of aluminium and copper in the solution (Fig. 1a).

Corrosion rate of the intermetallic phase, v_{corr}, was calculated on the basis of concentrations of aluminium and copper in the solution (Fig. 1b). It is possible to see that v_{corr} decreases as c_{inh} increases which suggests efficient corrosion inhibition in the studied system. However, this effect is partially related to the pH increase. For instance, acidification of the solution containing 100 mM of Na_3VO_4 from 1.11 to 0.76 increased the corrosion rate over 9-fold. Nevertheless, the corrosion rate is still much lower when compared to the uninhibited solution.

3.2. Electrochemical analysis

The open circuit potential (OCP) was determined as the preliminary step before further electrochemical analysis (Fig. 3).

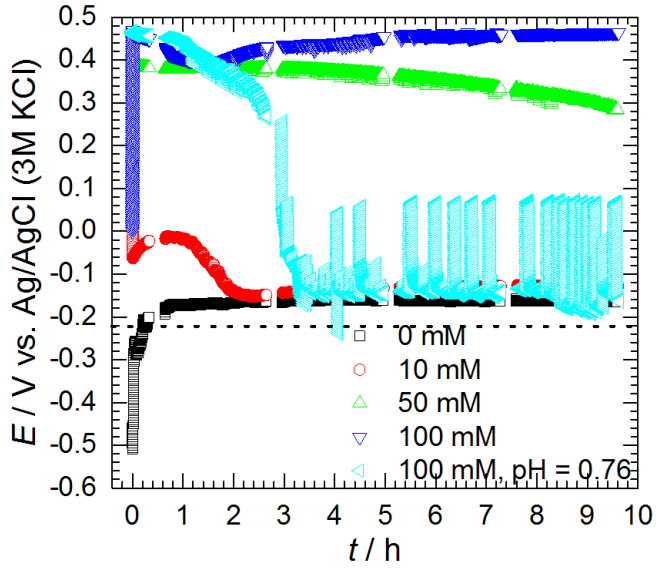

Fig. 3. Open circuit potential of Al_2Cu in 1 M H_3PO_4, T = 303 K, as a function of time and initial concentration of Na_3VO_4, dotted line indicates equilibrium potential of H_2 evolution

Al_2Cu initially corrodes via hydrogen and oxygen depolarisation. OCP increases with time, due to selective dissolution of aluminium, to the value, where hydrogen evolution is thermodynamically forbidden (dotted line in Fig. 3). Then, the corrosion mechanism changes to oxygen depolarisation. Sodium orthovanadate shifts the OCP anodically, when its concentration is sufficiently high (≥50 mM) which may indicate passivation of the Al_2Cu phase. When the pH of the solution containing 100 mM of Na_3VO_4 is set to 0.76, the OCP gradually decreases with time from the value obtained at pH = 1.11 to the level of the uninhibited solution. Moreover, its value oscillates with time. Probably it is related to formation and subsequent dissolution of a corrosion product on the surface of the intermetallic phase.

Polarisation curves were determined after 159 min immersion, where OCP value is too positive for hydrogen evolution. Thus, the cathodic process for uninhibited solution should be oxygen reduction (Fig. 4a). In aerated solution, there is also a possibility of mechanical detachment of porous copper structure, its chemical dissolution and subsequent reduction on the surface of the intermetallic phase. The cathodic current density initially remains low and when the overpotential is sufficiently cathodic $\eta < -0.30$ V, hydrogen evolution begins. Interestingly, when the solution is deaerated, cathodic current density is higher when compared to the previous case. This effect is reproducible. At the same time, rapid hydrogen evolution from deaerated solution occurs at lower overpotential when compared to the aerated one. The mechanism of cathodic process when the potential is above the equilibrium potential for hydrogen electrode remains unclear. First of all, it should be noted that current densities presented in Fig. 4 were obtained using the geometric value of the surface area, not the real one. It remains unknown and can be very high for selectively corroded specimens (c_{inh} = 0 and 10 mM). Thus, possible differences in the real surface area may also influence polarisation curves. Cathodic current flow might be related, incomplete deoxygenation of the solution or adsorption of hydrogen ions on the porous surface. Copper content on the surface, possibly higher in the deaerated solution and difference in the morphology of the porous, copper-rich layer may also affect cathodic polarisation curves.

When c_{inh} = 10 mM, the cathodic current increased when compared to c_{inh} = 0 mM (solutions in equilibrium with air). Sodium orthovanadate, when dissolved in orthophosphoric acid solution can form dark red-brown heteropolyoxovanadate species $HPV_{14}O_{42}^{9-}$. However, observed yellow colouration of the solutions indicates predominance of VO_2^+ cations [5]. In the corrosion cell, they are reduced at OCP to VO^{2+} and slightly green colouration of the solution appears. Standard reduction potential for this process E^0 = 1.0 V vs. standard hydrogen electrode (SHE) [19]. The subsequent reduction of VO^{2+} to V^{3+} is also possible at OCP (E^0 = 0.337 V vs. SHE) [19]. Therefore, vanadium species together with oxygen act as depolarisers in the corrosion cell and increases cathodic current density. When the solution was deaerated, current density decreased, as it was expected.

When c_{inh} = 50 mM, in aerated solution, VO_2^+ cations are reduced at OCP to VO^{2+}, but further reduction to V^{3+} is thermodynamically forbidden. On the cathodic polarisation curve, reduction of VO^{2+} to V^{3+} in the solution should occur around η = −0.23 V. Instead, oxidation peak is observed. It may suggest that the surface is covered with a protective layer, containing vanadium at +4 oxidation state, which prevents the charge transfer from metal to the solution, but undergoes oxidation. On the one hand, this layer is very thin since is not visible using SEM. On the other hand, in spot 2 (Fig. 2c) a small amounts of vanadium and phosphorus were detected, although no corrosion product is visible (Table 1). Such a layer can be responsible for corrosion inhibition of Al_2Cu phase in this solution. At $\eta < -0.80$ V, reduction of V^{3+} to V^{2+} occurs. Cathodic current density is significantly

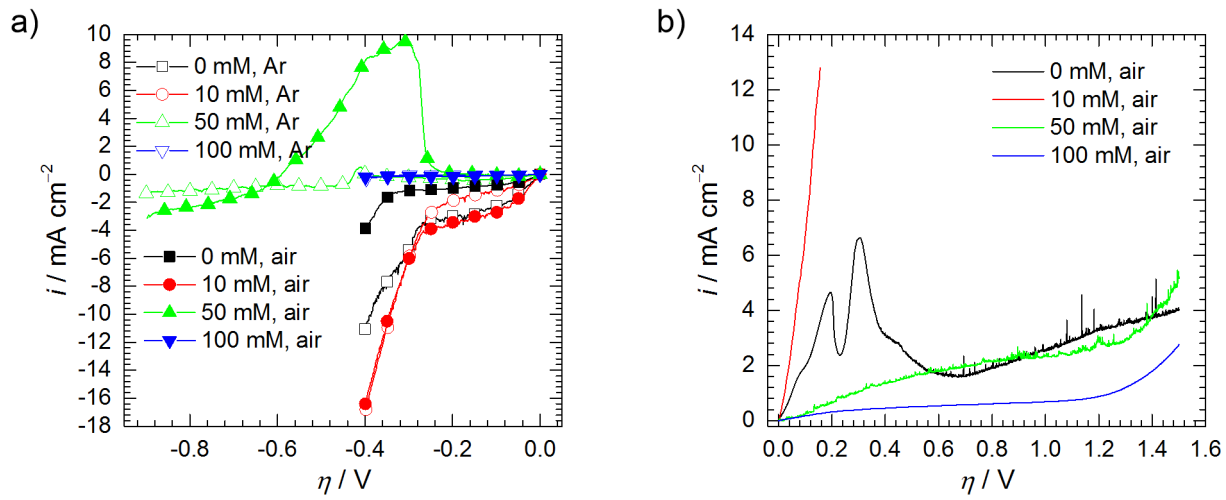

Fig. 4. Polarisation curves of Al_2Cu phase, obtained after $t = 159$ min of immersion in 1 M H_3PO_4, $T = 303$ K, as a function of initial concentration of Na_3VO_4, scanning rate was equal to 10 mV min^{-1}

lower when compared to the solutions containing 0 and 10 mM of Na_3VO_4, due to much lower surface area of the electrode (no selective corrosion occurred). Interestingly, in deaerated solution, the oxidation peak diminishes almost completely. This may suggest important, positive influence of oxygen on the corrosion resistance of Al_2Cu phase in this solution.

The lowest values of cathodic current densities were obtained for the solution containing 100 mM of Na_3VO_4, due to precipitation of the corrosion product (Fig. 1d, h and 3). Its thick layer inhibits the charge transfer from the electrode to depolariser in the solution. As it was expected, lower values of current density were obtained in the deaerated solution when compared to the aerated one. The insoluble salt precipitated on the surface contains vanadium and phosphorus; the V/P atomic ratio is close to unity. Vanadium should be on +4 oxidation state, since the open circuit potential was too high for further reduction of tetravalent vanadium species.

Anodic polarisation curve of Al_2Cu, in the solution containing 0 mM of Na_3VO_4, exhibits two current peaks (Fig. 4b). The first one, at $\eta = 0.20$ V, is probably oxidation of hydrogen molecules adsorbed onto the porous surface of selectively corroded specimen. The other one, at $\eta = 0.30$ V, is related to oxidation of copper. Then current density decreases, probably due to formation of insoluble copper(II) phosphate. Current density in the passive state is relatively high, it can be related to the high surface area of the electrode.

When $c_{inh} = 10$ mM, anodic current density is higher when compared to the uninhibited solution. However, the corrosion rate for the former case is lower. It means that the charge transfer between vanadium at various oxidation states occurs together with dissolution of the intermetallic phase (Fig. 4).

The anodic branch of polarisation curve, obtained for 50 mM of sodium orthovanadate, indicates spontaneous passivity of Al_2Cu phase, however the current density is relatively large. Much lower values are observed in the solution containing 100 mM of Na_3VO_4, due to thick, protective layer of insoluble salt deposited onto the surface.

Electrochemical impedance spectroscopy (EIS) was used to study the influence of the chemical composition of the solutions on the corrosion mechanism of Al_2Cu. (Fig. 5). When $c_{inh} \leq 10$ mM, the imaginary part of the impedance decreases, as the frequency decreases, in the range between 200 and 10 kHz. It is related to the formation of porous, copper-rich layer on the surface of the electrode [20]. However, some contribution from the experimental setup (e.g. impedance of the reference electrode and the input capacitance of the voltage amplifier of potentiostat) cannot be excluded [21]. The increase of $|Z''|$ with decreasing frequency, marked with straight line, is related to the double layer capacitance connected in parallel to the charge transfer resistance. This part of the spectrum, for severely corroded specimens, is preceded by a short, linear part, characterised with low slope, also related to the porosity of the electrode. In this work, the impedance response related to the porosity of the electrode

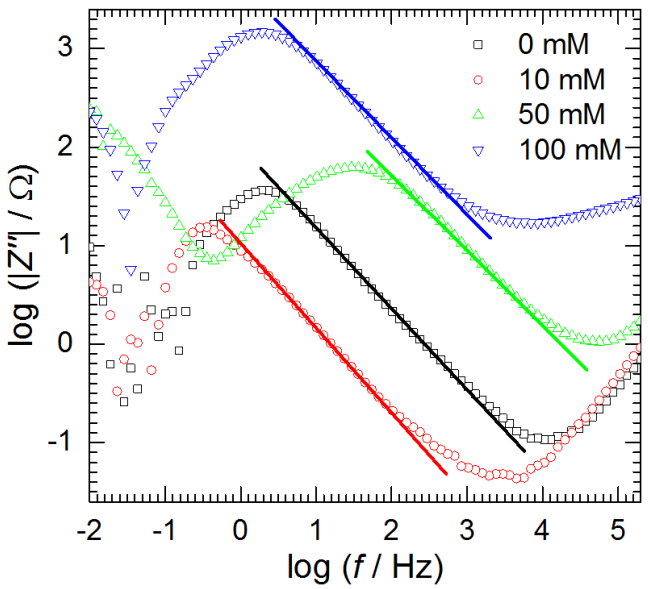

Fig. 5. Modulus of the imaginary part of impedance as a function of frequency and initial concentration of Na_3VO_4, 1 M H_3PO_4, $t = 576$ min, $T = 303$ K

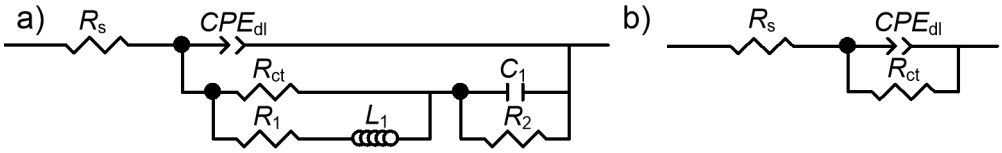

Fig. 6. Electrical equivalent circuits used for approximation of impedance spectra

was excluded from approximation. In the low frequency range ($f < 1$ Hz, for 50 mM of Na_3VO_4 $f < 30$ Hz), two additional time constants appear. They are well defined for the solutions containing ≥10 mM of Na_3VO_4 and can be attributed to the adsorption of the intermediate species during anodic and cathodic (vanadium (V) reduction) processes in the corrosion cell.

Impedance spectra were approximated using two electrical equivalent circuits (EECs) (Fig. 6) and the values of the electrical components of EEC were obtained (Table 2 and 3). The influence of the initial concentration of sodium orthovanadate and the immersion time on the charge transfer resistance R_{ct} and the double layer capacitance C_{dl} was established.

In both models, a constant phase element CPE_{dl} was applied instead of the capacitor to describe the capacitance of the electrode double layer. Its impedance is given by equation:

$$Z_{CPE} = \frac{1}{T(j\omega)^{\alpha}} \tag{2}$$

where ω is the frequency and $\alpha < 1$ indicates the deviation from the capacitive behaviour. The Brug's equation was applied to calculate the double layer capacitance [22]:

$$C_{dl} = T_{dl}^{\frac{1}{\alpha}} \left(\frac{1}{R_s} + \frac{1}{R_{ct}} \right)^{1-\frac{1}{\alpha}} \tag{3}$$

where R_s is the solution resistance and R_{ct} is the charge transfer resistance. This equation works well, when $\alpha > 0.85$. Otherwise, uncertainty of C_{dl} calculation can be significant [23]. The inductive and capacitive loops, related to the adsorption processes, were approximated using inductor L_1 in series with R_1 and the

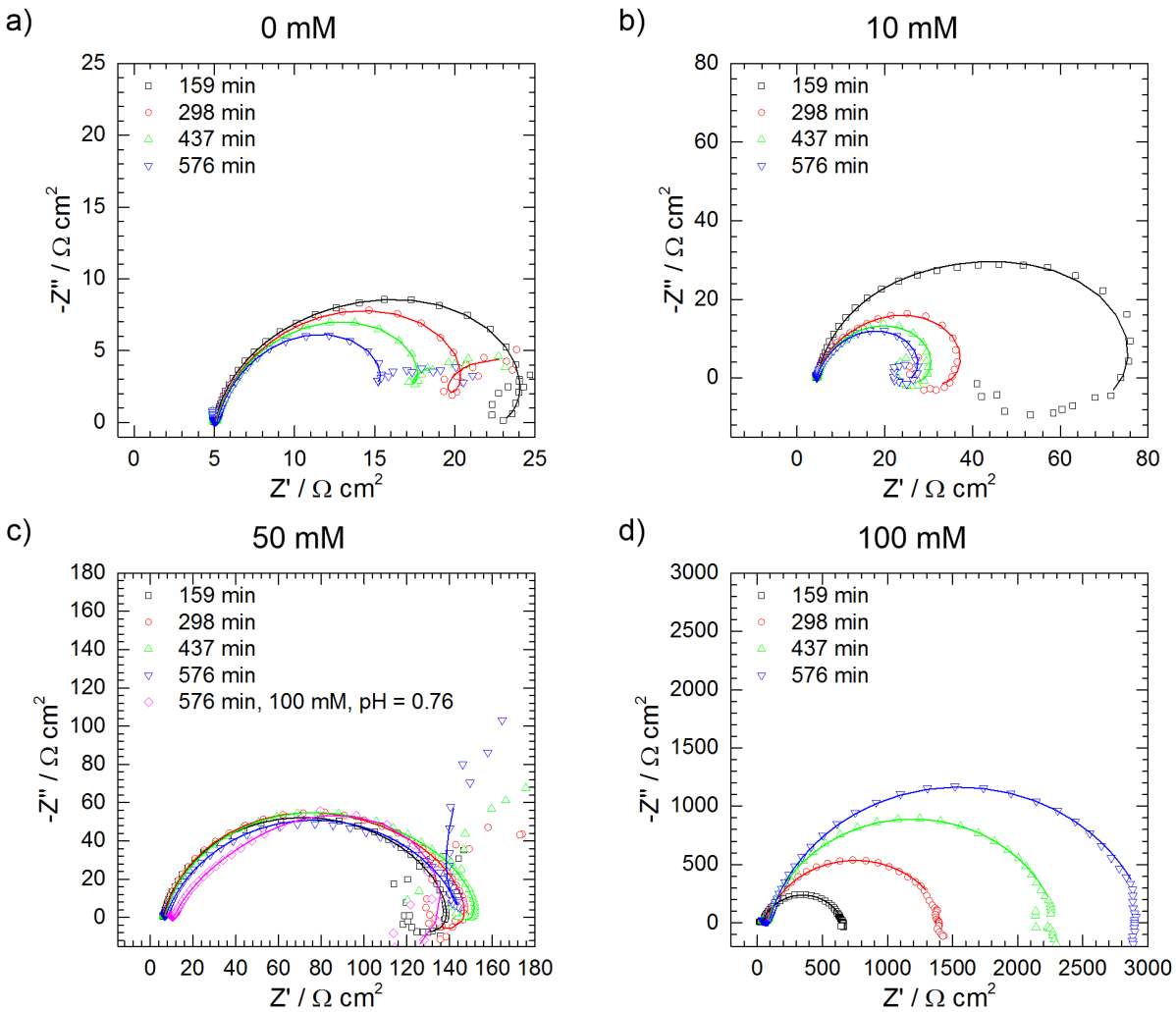

Fig. 7. Nyquist plots for the corrosion of Al_2Cu as a function of time and initial concentration of Na_3VO_4 in 1 M H_3PO_4, $T = 303$ K, continuous lines represent approximation of the data obtained

capacitor C_1 in parallel with R_2 (Fig. 6a). The EEC applied for $c_{inh} < 100$ mM was introduced by Cao [24] for the system where two potential dependent processes (e.g. adsorption of two different species) occurs at the surface of the electrode, besides the charge transfer. R_1 and L_1. can be related to the adsorption of intermediate species due to the anodic dissolution of metal and/or corrosion inhibitor species. The former takes into account the kinetics of changes to the fractional surface coverage or film resistivity with time. The latter is related to the time constant of this process C_1 and R_2 are related to the charge-transfer resistance, the change in the electric current passing through the interface caused by a change in the fractional coverage of the surface, film resistivity, or thickness, as well as the time constants related to these processes [24,25]. The results of approximation of the impedance spectra with this EEC are presented in Table 2.

Aforementioned equivalent circuit was not applicable for the impedance spectra obtained for the highest initial concentration of sodium orthovanadate. These were approximated using a simple, Randles-type model (Fig. 6b). Although more than one time constant, besides the response related to the porous layer of corrosion product, is observed, such a simple model gives relatively good fit quality and enables determination of the double layer capacitance and the charge transfer resistance. The results of approximation of the impedance spectra with this EEC are presented in Table 3.

The impedance of Al_2Cu phase decreases with immersion time for $c_{inh} \leq 10$ mM due to the selective corrosion. However it can be seen that Na_3VO_4 slightly inhibits this process (higher values of impedance in Fig. 7b than a).

When the concentration of sodium orthovanadate is 50 mM, the impedance spectra virtually do not change with the immersion time, and the impedance is higher when compared to the two previous cases (Fig. 7c). Moreover, the shape of the impedance spectra, according to Epelboin et al., indicates passivation of the electrode [25].

Finally, for c_{inh} = 100 mM, the highest impedance values were obtained. They also increase with the immersion time due to continuous precipitation of the corrosion products on the surface of the electrode (Fig. 5d). However, when this solution was acidified to pH = 0.76, there was no precipitation of the corrosion product and much lower values of impedance were measured, comparable to those obtained in the solution containing 50 mM of Na_3VO_4 (Fig. 7c). Impedance spectra for $t < 576$ min were not analysed due to OCP oscillations during measurement (Fig. 3).

Double layer capacitance is a good indicator of the selective corrosion. It increases with immersion time due to increase of the surface area of the electrode. Thus, the higher value of C_{dl}, the more severely corroded surface is (Fig. 8a). Capacitances presented in this work (Table 2, Fig. 8a) are divided by the geometric surface area of the electrode, not the real one, which remains unknown. The selective corrosion was supressed when $c_{inh} \geq 50$ mM. Double layer capacitance is then stable over time, within the range of 17 – 18 mF cm^{-2} for 50 mM and 9 – 11 mF cm^{-2} for 100 mM of Na_3VO_4.

Charge transfer resistance is small and decreases over time in those solutions, where selective corrosion occurs ($c_{inh} \leq 10$ mM, Fig. 6b), due to increase of the surface area of the electrode. Again, reported value are multiplied by the geometric value of surface area, not the real one. A weak, temporary corrosion inhibition occurs for c_{inh} = 10 mM, but this effect diminishes when $t \geq 159$ min. In the solution containing 50 mM of Na_3VO_4 the electrode becomes passive. R_{ct} values are stable over time, but relatively small. Probably the solution is too aggressive and the passive layer is very thin and unstable. The high values of current density in the passive state confirms this assumption. R_{ct} again depends on the immersion time for the highest concentration of sodium orthovanadate (100 mM). In this case it increases due to build-up of the protective layer on the surface.

Inhibition efficiency was calculated according to equation:

$$P = \left(1 - \frac{v_{corr,inh}}{v_{corr,0}}\right) \cdot 100\% \qquad (4)$$

where $v_{corr,0}$ and $v_{corr,inh}$ stand for the corrosion rate determined in uninhibited and inhibited solutions respectively. Inhibition efficiency reaches 78% for c_{inh} = 50 and 99% for c_{inh} = 100 mM.

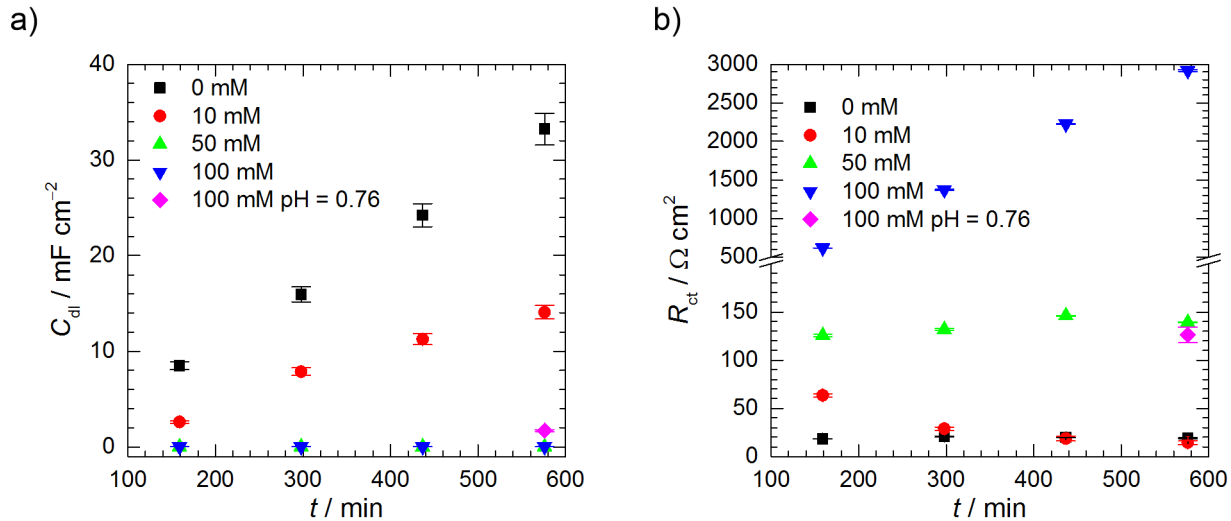

Fig. 8. Corrosion kinetics of Al_2Cu in 1 M H_3PO_4, T = 303 K: a) double layer capacitance and b) charge transfer resistance

TABLE 2

The results of approximation of the impedance spectra, χ^2 and S indicate the quality of the fit (chi-square and residual sum of squares respectively)

c_{inh} (mM)	t (min)	χ^2	S	R_s (Ω cm^2)	ΔR_s (%)	T_{dl} (mF s^{a-1} cm^{-2})	ΔT_{dl} (%)	α_{dl}	$\Delta\alpha_{dl}$ (%)	R_{ct} (Ω cm^2)	ΔR_{ct} (%)	L_1 (H cm^2)	ΔL_1 (%)	R_1 (Ω cm^2)	ΔR_1 (%)	C_1 (mF cm^{-2})	ΔC_1 (%)	R_2 (Ω cm^2)	ΔR_2 (%)
0 mM	159	$6.51\ 10^{-5}$	0.004	5.1	0.1	12.183	1.5	0.89	0.4	18.3	2.0	66.8	12.5	42.9	9.1	60.741	9.9	4.6	8.3
	298	$3.14\ 10^{-4}$	0.024	5.1	0.2	24.057	1.3	0.85	0.6	20.8	1.6	62.7	5.4	38.3	5.8	849.886	8.5	8.6	3.2
	437	$6.76\ 10^{-5}$	0.005	5.1	0.1	33.863	0.8	0.86	0.4	19.7	1.4	36.7	3.1	27.4	4.3	634.278	7.1	7.7	2.4
	596	$3.67\ 10^{-5}$	0.002	5.2	0.1	44.091	1.0	0.86	0.4	19.0	2.4	21.8	4.3	23.0	3.9	695.975	9.7	10.7	26.9
10 mM	159	$5.77\ 10^{-4}$	0.036	4.7	0.7	4.053	2.2	0.90	0.6	63.5	2.9	287.1	13.9	63.2	30.4	24.705	13.1	21.4	9.5
	298	$3.68\ 10^{-4}$	0.023	4.6	0.4	10.774	3.2	0.91	1.0	28.7	5.9	48.8	17.5	13.7	31.6	20.194	10.9	16.8	12.6
	437	$5.56\ 10^{-4}$	0.033	4.6	0.6	14.558	7.0	0.92	2.0	18.5	13.6	32.8	20.0	6.6	50.1	14.443	11.7	15.8	12.0
	576	$4.39\ 10^{-4}$	0.027	4.6	0.4	17.642	6.6	0.93	1.8	14.3	13.0	22.8	18.0	2.7	70.4	13.899	7.3	16.3	8.0
50 mM	159	$2.41\ 10^{-4}$	0.025	6.2	0.2	0.054	1.4	0.88	0.2	125.6	0.8	531.9	6.2	782.3	7.4	1.119	21.5	8.7	10.8
	298	$1.61\ 10^{-4}$	0.015	6.5	0.2	0.053	1.2	0.88	0.2	131.7	0.6	573.0	6.8	1008.0	4.8	1.016	14.2	11.1	7.0
	437	$8.43\ 10^{-4}$	0.089	6.7	0.5	0.073	1.4	0.84	0.2	146.1	0.3	1088.6	8.3	1120.2	10.4	111.237	4.2	187.0	15.5
	596	$5.65\ 10^{-4}$	0.061	7.0	0.5	0.107	1.4	0.80	0.3	139.3	0.3	1825.7	11.8	1341.4	26.7	59.337	5.3	463.8	33.8
100 mM pH = 0.76	159																		
	298																		
	437																		
	576	$3.87\ 10^{-4}$	0.026	11.0	0.5	4.732	2.6	0.75	0.9	126.2	6.5	210.4	4.2	1.0	50	5.2185	11.7	71.5	4.1

TABLE 3

The results of approximation of the impedance spectra, χ^2 and S indicate the quality of the fit (chi-square and residual sum of squares respectively)

c_{inh} (mM)	t (min)	χ^2	S	R_s (Ω cm^2)	ΔR_s (%)	T_{dl} (mF s^{a-1} cm^{-2})	ΔT_{dl} (%)	α_{dl}	$\Delta\alpha_{dl}$ (%)	R_{ct} (Ω cm^2)	ΔR_{ct} (%)
100 mM	159	$3.51\cdot10^{-4}$	0.0231	41.2	0.7	0.054	1.3	0.84	0.3	617.3	0.4
	298	$3.98\cdot10^{-4}$	0.0231	66.3	0.8	0.046	1.4	0.84	0.3	1373.0	0.7
	437	$2.63\cdot10^{-4}$	0.0173	80.0	0.7	0.042	0.8	0.86	0.2	2227.0	0.4
	596	$2.60\cdot10^{-4}$	0.0172	89.1	0.6	0.042	0.8	0.86	0.2	2918.3	0.4

However, this effect is due to pH shift of the solutions. When c_{inh} = 100 mM, at pH stabilised at 0.76 inhibition efficiency was also equal to 76%.

4. Summary

Sodium orthovanadate was tested as the corrosion inhibitor of intermetallic Al_2Cu in 1 M H_3PO_4. It can be concluded that when its concentration is equal to 50 mM, corrosion inhibition is achieved to some extent, due to passivation of the electrode. However much better effect was obtained for c_{inh} = 100 mM due to precipitation of the compact, protective layer on the surface of Al_2Cu phase. This process occurs in the well-defined range of pH, because, when the solution containing 100 mM of sodium orthovanadate was acidified to pH = 0.76, there was no precipitation of the protective layer.

On the one hand, precipitation of the stable corrosion product is undesirable in terms of gravimetric determination of the weight of anodic coating. On the other hand, its formation on the surface of Al_2Cu intermetallic phase can be interesting from the point of view of deposition of conversion coatings onto copper rich aluminium alloys.

Acknowledgment

The financial support from the National Science Centre, Poland, Grant No. 2016/23/D/ST5/01343 is gratefully acknowledged. The authors also gratefully acknowledge Dr. Dariusz Szeliga and Mr. Andrzej Gradzik for preparing the Al_2Cu intermetallic phase, Dr. Barbara Kościelniak for her help in microscopic analysis, and Mr. Kamil Dychtoń for his help in conducting the electrochemical research.

REFERENCES

[1] N.A. Belov, D.G. Eskin, A.A. Aksenov, Multicomponent phase diagrams: applications for commercial aluminum alloys, Elsevier, Oxford (2005).

[2] J.R. Scully, T.O. Knight, R.G. Buchheit, D.E. Peebles, Electrochemical characteristics of the Al_2Cu, Al_3Ta and Al_3Zr intermetallic phases and their relevancy to the localized corrosion of Al alloys, Corros Sci. **35**, 185-195 (1993).

[3] R.G. Buchheit, A compilation of corrosion potentials reported for intermetallic phases in aluminum alloys, J Electrochem Soc. **142**, 3994-3996 (1995).

[4] ASTM B137-95, Standard Test Method for Measurement of Coating Mass Per Unit Area on Anodically Coated Aluminum, (2009).

[5] M.T. Pope, Heteropoly and Isopoly Oxometalates, Springer-Verlag, Berlin (1983).

[6] P. Kwolek, A. Kamiński, K. Dychtoń, M. Drajewicz, J. Sieniawski, The corrosion rate of aluminium in the orthophosphoric acid solutions in the presence of sodium molybdate, Corros Sci. **106**, 208-216 (2016).

[7] X. Li, S. Deng, H. Fu, Sodium molybdate as a corrosion inhibitor for aluminium in H_3PO_4 solution, Corros Sci. **53**, 2748-2753 (2011).

[8] K. Dychtoń, P. Kwolek, The replacement of chromate by molybdate in phosphoric acid-based etch solutions for aluminium alloys, Corros Eng Sci Technol. **53**, 234-240 (2018).

[9] P. Kwolek, M. Wojnicki, Spectrophotometric study of corrosion inhibition of aluminium in orthophosphoric acid aqueous solutions by using sodium molybdate, Corros Eng Sci Technol. **54**, 199–204 (2018).

[10] P. Kwolek, A. Pustuła, W.J. Nowak, Influence of molybdophosphoric acid on the kinetics of the anodic coating dissolution, Surf Coatings Technol. **357**, 535–542 (2019).

[11] M. Iannuzzi, G.S. Frankel, Mechanisms of corrosion inhibition of AA2024-T3 by vanadates, Corros Sci. **49**, 2371-2391 (2007).

[12] K.D. Ralston, S. Chrisanti, T.L. Young, R.G. Buchheit, Corrosion Inhibition of Aluminum Alloy 2024-T3 by Aqueous Vanadium Species, J Electrochem Soc. **155**, C350-C359 (2008).

[13] K.D. Ralston, T.L. Young, R.G. Buchheit, Electrochemical Evaluation of Constituent Intermetallics in Aluminum Alloy 2024-T3 Exposed to Aqueous Vanadate Inhibitors, J Electrochem Soc. **156**, C135-C146 (2009).

[14] K.D. Ralston, R.G. Buchheit, An Initial Exploration of Corrosion Inhibition of AA6061 and AA7075 by Aqueous Vanadates, ECS Electrochem Lett. **2**, C35-C38 (2013).

[15] D.S. Kharitonov, J. Sommertune, C. Örnek, J. Ryl, I.I. Kurilo, P.M. Claesson, J. Pan, Corrosion Inhibition of Aluminium Alloy AA6063-T5 by Vanadates: Local Surface Chemical Events Elucidated by Confocal Raman Micro-Spectroscopy, Corros Sci. **148**, 237-250 (2018).

[16] B. Boukamp, A linear Kronig-Kramers transform test for immittance data validation, J Electrochem Soc. **142**, 1885-1894 (1995).

[17] B. Boukamp, Electrochemical impedance spectroscopy in solid state ionics: recent advances, Solid State Ionics. **169**, 65-73 (2004).

[18] N. Birbilis, R.G. Buchheit, Investigation and discussion of characteristics for intermetallic phases common to aluminum alloys as a function of solution pH, J Electrochem Soc. **155**, C117-C126 (2008).

[19] C.G. Zoski, Handbook of Electrochemistry, Elsevier, Amsterdam (2007).

[20] I. Frateur, C. Deslouis, M.E. Orazem, B. Tribollet, Modeling of the cast iron / drinking water system by electrochemical impedance spectroscopy, Electrochim Acta. **44**, 4345-4356 (1999).

[21] A.-T. Tran, F. Huet, K. Ngo, P. Rousseau, Artefacts in electrochemical impedance measurement in electrolytic solutions due to the reference electrode, Electrochim Acta. **56**, 8034-8039 (2011).

[22] B. Hirschorn, M.E. Orazem, B. Tribollet, V. Vivier, I. Frateur, M. Musiani, Determination of effective capacitance and film thickness from constant-phase-element parameters, Electrochim Acta. **55**, 6218-6227 (2010).

[23] B. Łosiewicz, R. Jurczakowski, A. Lasia, Kinetics of hydrogen underpotential deposition at iridium in sulfuric and perchloric acids, Electrochim Acta. **225**, 160-167 (2017).

[24] C. Cao, On the impedance plane displays for irreversible electrode reactions based on the stability conditions of the steady state II. Two state variables besides electrode potential, Electrochim Acta. **35**, 837-844 (1990).

[25] I. Epelboin, C. Gabrielli, M. Keddam, H. Takenouti, The Study of the Passivation Process by the Electrode Impedance Analysis, in: J. Bockris, B.E. Conway, E. Yeager, R.E. White (Eds.), Electrochem Mater Sci Compr Treatise Electrochem, Springer, Boston MA (1981).